Nanoscale

RSCPublishing

ARTICLE

Supplementary information

Comprehensive and quantitative analysis for controlling the physical/chemical states and particle properties of nanodiamonds for biological applications

S. Sotoma[a], K. Akagi[b], S. Hosokawa[a,c], R. Igarashi[a], H. Tochio[d], Y. Harada[e] and M. Shirakawa[a,*]

[a]*Department of Molecular Engineering, Graduate School of Engineering, Kyoto University, Nishikyo-ku, Kyoto 615-8510, Japan.*
[b]*Section of Laboratory Equipment, National Institute of Biomedical Innovation, 7-6-8 Saito Asagi Ibaraki-city, Osaka, 567-0085, Japan.*
[c]*Elements Strategy Initiative for Catalysts & Batteries (ESICB), Kyoto University, Kyotodaigaku Katsura, Nishikyo-ku, Kyoto 615-8520, Japan*
[d]*Department of Biophysics, Graduate School of Science, Kyoto University, Kitashirakawa-oiwake, Sakyo-ku, Kyoto 606-8502, Japan.*
[e]*Institute for Integrated Cell-Material Sciences (WPI-iCeMS), Kyoto University, Yoshida-Honmachi, Sakyo-ku, Kyoto 606-8501, Japan*

**Corresponding author*
E-mail: shirakawa@moleng.kyoto-u.ac.jp

Figure S1. Precisely measured XRD spectra for the (111) diffraction patterns of ND-pris (brown), ND-800 (orange), ND-500 (green), ND-550 (blue), and ND-600 (red).

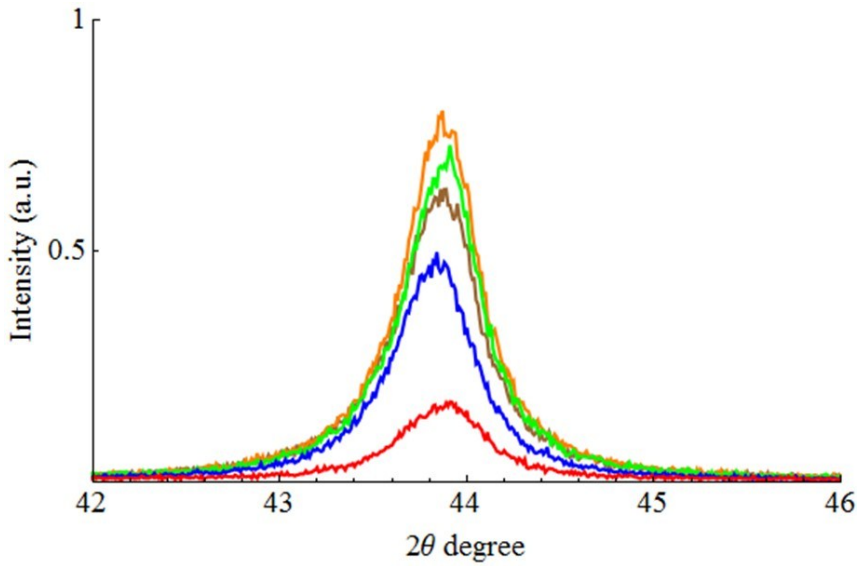

Figure S2. Ratios of oxygen to carbon in ND samples estimated based on elemental analysis (squares) and XPS (triangles) results.

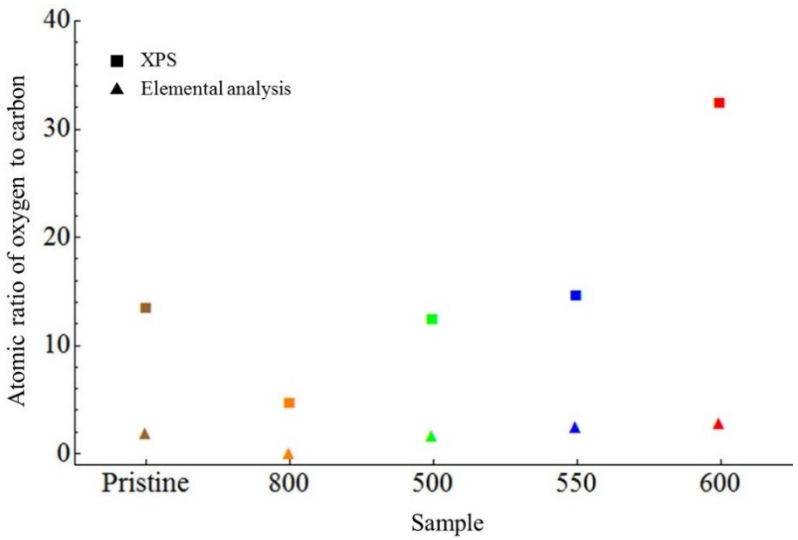

Figure S3. Survey XPS spectra of ND samples. The Ag 3d orbital was used as an internal standard.

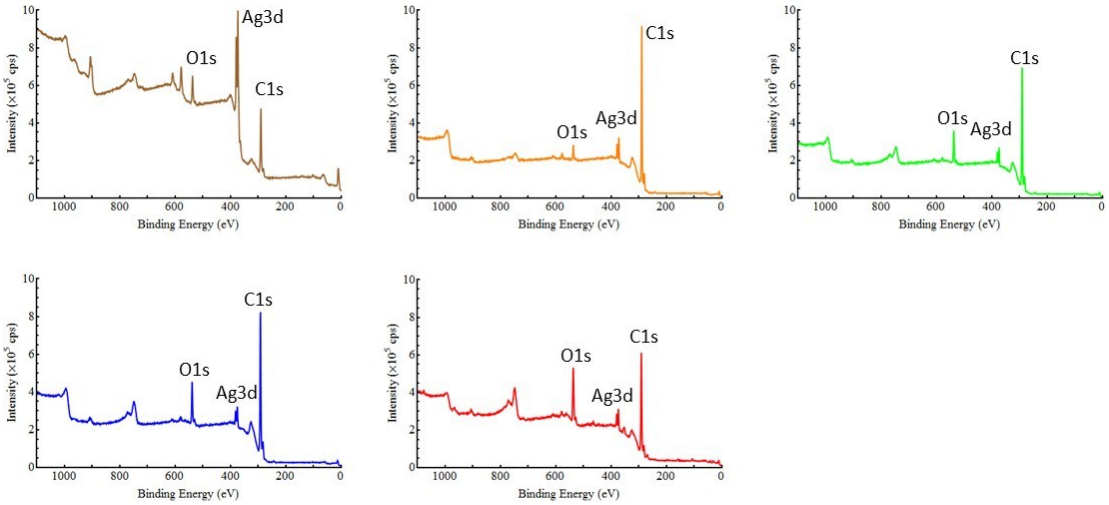

Figure S4. Ratios of the sp^3 to sp^2 bonds in the ND samples estimated from their Raman and XPS spectra.

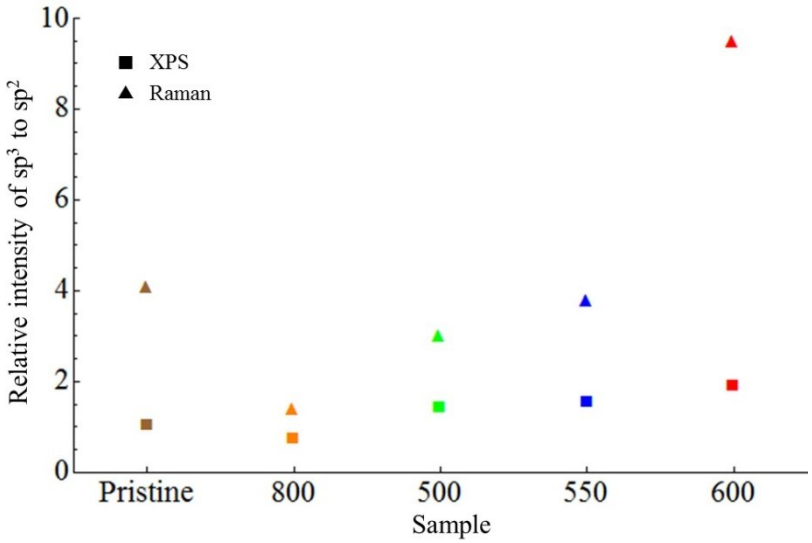

Figure S5. Dispersion state of ND-800. This sample immediately precipitated in water prior to analysis, thus the proper experimental data was not obtained.

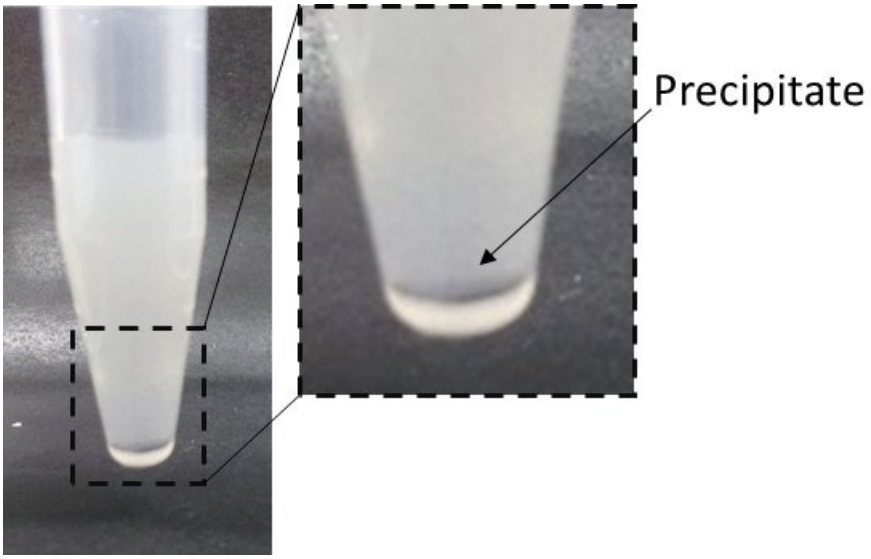

Figure S6. (a) Deconvoluted high-resolution O1s XPS spectra of the ND samples along with a comparison plot of each component for all of the samples. As was done for the C1s XPS spectra, each spectrum was curve-fitted into three peak components with binding energies of 529.5 ± 0.5, 531 ± 1.0, and 533 ± 1.0 eV, which were attributed to OH, C=O, and COOH bonding groups. Table 3 lists the existence probability of each component in the ND samples. Not surprisingly, COOH groups were the least likely for ND-800. In the subsequent oxidation process, it was anticipated that the COOH component would increase with increasing temperature. However, when comparing ND-550 to ND-600, the increase in the COOH concentration was very small, while the content of C=O groups was highly enhanced. These results support the dehydration of surface carboxyl groups which stated in the main text.

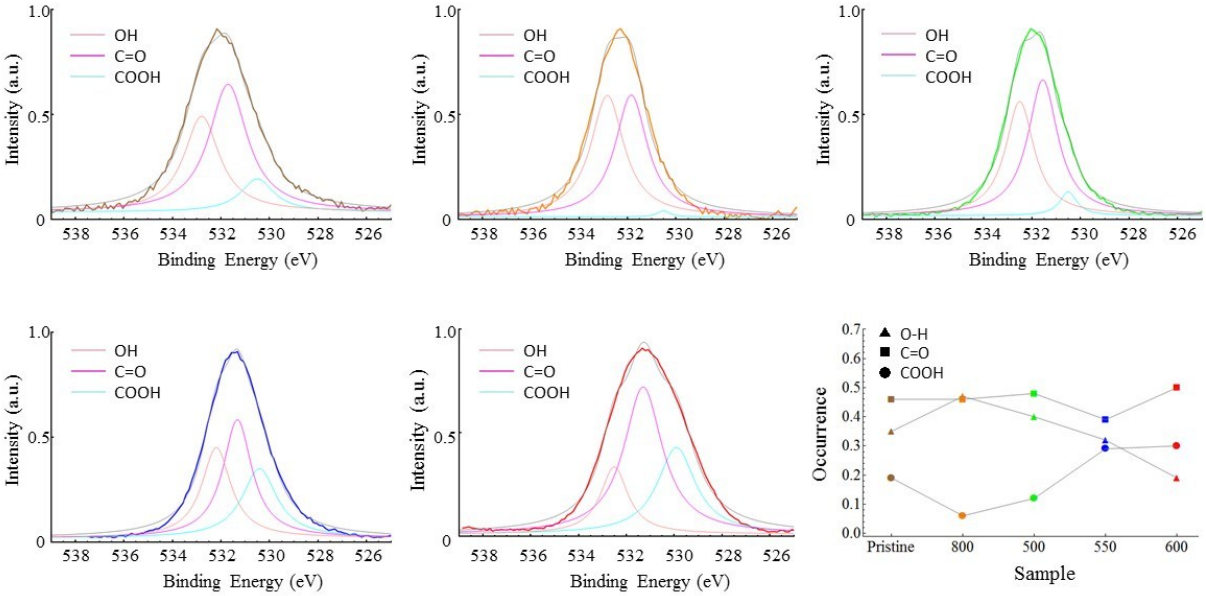

Figure S7. Time-dependent changes in the dispersion state of NDs in NaCl solutions with different concentrations.

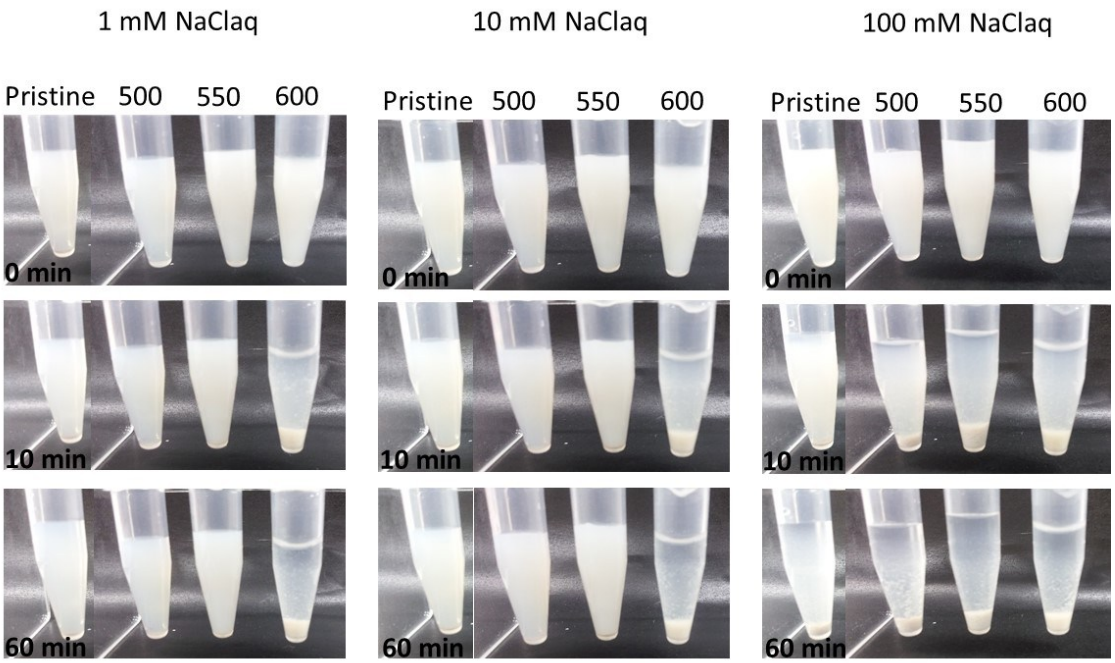

Figure S8. Surface distance versus the solid fraction for ND-pris (brown), ND-800 (orange), ND-500 (green), ND-550 (blue), and ND-600 (red) calculated using Woodcock's theory (Woodcock L. V., *Lect. Notes Phys*. 1987, 277, 113).

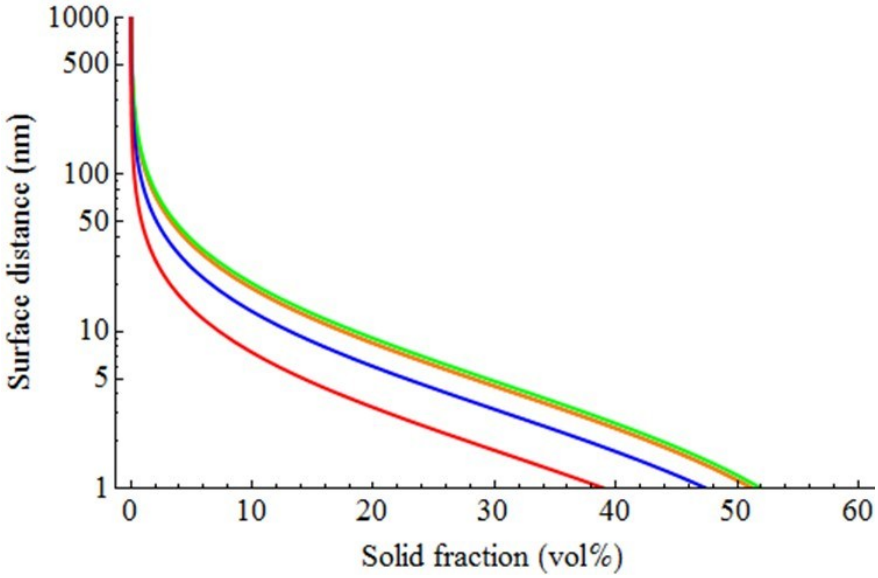

Figure S9. Particle-size distribution of dispersible ND samples measured by DLS (brown: ND-pris; green: ND-500; blue: ND-550). The Median size are similar to the size estimated by TEM images, however, distribution shows larger values than that of TEM. This large distribution of DLS might be caused by a certain level of aggregation of ND particles.

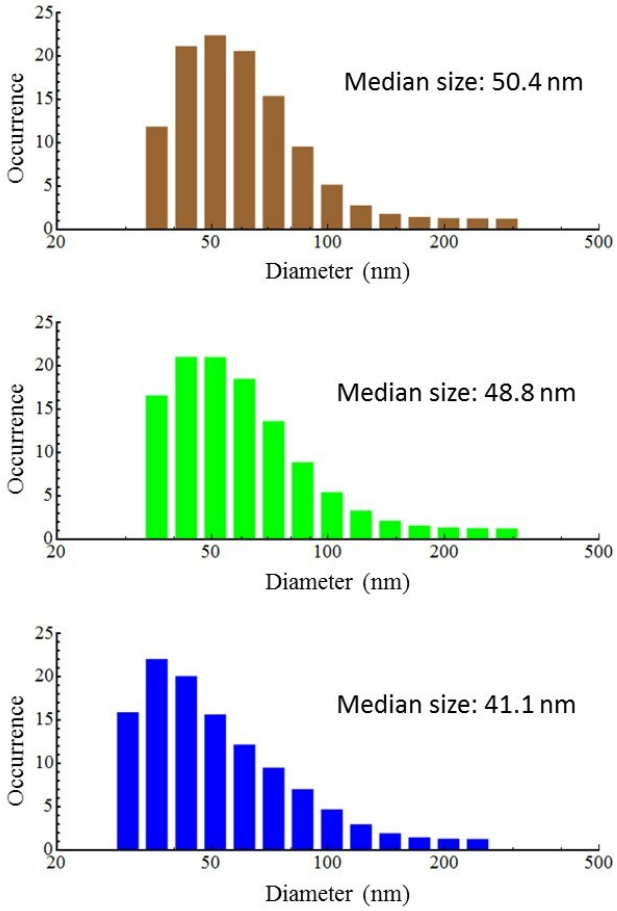

Table S1. Bragg angles and FWHMs of the (111) peaks of the ND samples in Figure S1 determined via Lorenzian fitting and their crystal sizes are estimated using Scherrer's equation. As the values of crystallite size of ND-550 and ND-600 are larger than the particle size estimated from TEM images (Figure 3), these values are supposed to be inappropriate. This might be because that Scherrer's equation does not apply to particles with unusual shapes and containing crystal distortion, such as the NDs used in this study.

Parameter	Bragg angle (°)	FWHM (°)	Crystallite size (nm)
ND-pris	43.85	2.52	41.0
ND-800	43.87	2.36	44.3
ND-500	43.87	2.37	43.9
ND-550	43.82	2.44	42.6
ND-600	43.87	2.46	42.0

Table S2. Existence probabilities of the COOH, C=O, and OH components estimated from Figure 5a.

Component	COOH	C=O	OH
ND-pris	0.19	0.46	0.35
ND-800	0.06	0.46	0.47
ND-500	0.12	0.48	0.40
ND-550	0.29	0.39	0.32
ND-600	0.30	0.50	0.19